

A 3-Fluoro-4-hexylthiophene-Based Wide Bandgap Donor Polymer for 10.9% Efficiency Eco-Friendly Nonfullerene Organic Solar Cells

Jeong Eun Yu, Sung Jae Jeon, Jun Young Choi, Yong Woon Han, Eui Jin Ko, and Doo Kyung Moon*

Nonfullerene organic solar cells (NFOSCs) are attracting increasing academic and industrial interest due to their potential uses for flexible and lightweight products using low-cost roll-to-roll technology. In this work, two wide bandgap (WBG) polymers, namely P(fTh-BDT)-C6 and P(fTh-2DBDT)-C6, are designed and synthesized using benzodithiophene (BDT) derivatives. Good oxidation stability and high solubility are achieved by simultaneously introducing fluorine and alkyl chains to a single thiophene (Th) unit. Solid P(fTh-2DBDT)-C6 films present WBG optical absorption, suitable frontier orbital levels, and strong π - π stacking effects. In addition, P(fTh-2DBDT)-C6 exhibits good solubility in both halogenated and nonhalogenated solvents, suggesting its suitability as donor polymer for NFOSCs. The P(fTh-2DBDT)-C6:3,9-bis(2-methylene-(3-(1,1-dicyanomethylene)-indanone))-5,5,11,11-tetrakis(5-hexylthienyl)-dithieno[2,3-d:2',3'-d']-s-indaceno[1,2-b:5,6-b']dithiophene (ITIC-Th) based device processed using chlorobenzene/1,8-diiodooctane (CB/DIO) exhibits a remarkably high power conversion efficiency (PCE) of 11.1%. Moreover, P(fTh-2DBDT)-C6:ITIC-Th reaches a high PCE of 10.9% when processed using eco-friendly solvents, such as *o*-xylene/diphenyl ether (DPE). The cell processed using CB/DIO maintains 100% efficiency after 1272 h, while that processed using *o*-xylene/DPE presents a 101% increase in efficiency after 768 h and excellent long-term stability. The results of this study demonstrate that simultaneous fluorination and alkylation are effective methods for designing donor polymers appropriate for high-performance NFOSCs.


Organic solar cells (OSCs), which can be produced using solution processing, have been promising candidates in the field of photovoltaic conversion because they offer advantages such as light weight and affordability, they require simple solution process, and present device flexibility.^[1,2] In the past two decades, high-performance low bandgap donor polymers were

developed to achieve high-efficiency OSCs based on fullerene acceptors such as [6,6]-phenylC₇₁butyric acid methyl ester (PC₇₁BM).^[3-6] However, fullerene acceptors present significant disadvantages, such as morphological instability and limited synthetic control over their electronic and structural properties, which cause difficulty in controlling their energy levels and limit their light absorption ranges.^[7-9] To overcome these issues, nonfullerene OSCs (NFOSCs) using nonfullerene acceptors (NFAs) for increased stability and efficiency have been extensively studied.^[10-13] Recently, rapid advances in the field of NFAs, particularly synthesizing acceptor-donor-acceptor (A-D-A)-type molecules such as 3,9-bis(2-methylene-(3-(1,1-dicyanomethylene)-indanone))-5,5,11,11-tetrakis(4-hexylphenyl)-dithieno[2,3-d:2',3'-d']-s-indaceno[1,2-b:5,6-b']-dithiophene (ITIC)^[14] and 3,9-bis(2-methylene-(3-(1,1-dicyanomethylene)-indanone))-5,5,11,11-tetrakis(5-hexylthienyl)-dithieno[2,3-d:2',3'-d']-s-indaceno[1,2-b:5,6-b'] dithiophene (ITIC-Th)^[15] with indaceno-dithiophene (IDT) derivatives donors, have reached power conversion efficiencies (PCEs) of over 14%,^[16,17] and

their practical applications are now in demand.^[18-20] Unlike fullerene derivatives, which exhibit isotropic charge transfer, the conjugated backbones of NFAs are planar. This promotes intermolecular interactions and π - π stacking, thereby leading to good charge transport,^[15] and a high absorption coefficient was achieved in the wide wavelength range of 600–800 nm or higher. Thus, a wide bandgap (WBG) polymer with a complementary absorption range and well-matched energy levels would be advantageous for NFAs with low bandgaps.

It is most effective to control the properties of polymers by substituting the main backbone with fluorine atoms^[21-24] and ring substituents^[25-27] when designing donor polymers suitable for NFOSCs.^[28,29] In particular, introducing fluorine lowers the energy level of the highest occupied molecular orbital (HOMO) without affecting the energy bandgap, thus conferring the fluorinated polymers higher oxidation stability compared to that of

J. E. Yu, S. J. Jeon, J. Y. Choi, Y. W. Han, E. J. Ko, Prof. D. K. Moon
Nano and Information Materials (NIMs) Laboratory
Department of Materials Chemistry and Engineering
Konkuk University
120 Neungdong-ro, Gwangjin-gu, Seoul 05029, Korea
E-mail: dkmoon@konkuk.ac.kr

 The ORCID identification number(s) for the author(s) of this article can be found under <https://doi.org/10.1002/smll.201805321>.

DOI: 10.1002/smll.201805321

nonfluorinated polymers.^[30,31] In addition, the strong electronegativity of fluorine can enhance intramolecular and intermolecular interactions and increase charge-carrier mobility.^[32] In recent years, Beaujuge and co-workers used benzo[1,2-*b*:4,5-*b'*]dithiophene (BDT) and thiophene (Th) as polymer backbones, and synthesized three types of polymers with differing degrees of planarity and fluorination. Among them, PBDT(Th)[2F]T with a planar backbone and substituted 2Fs presented the highest PCE of 9.8%.^[33]

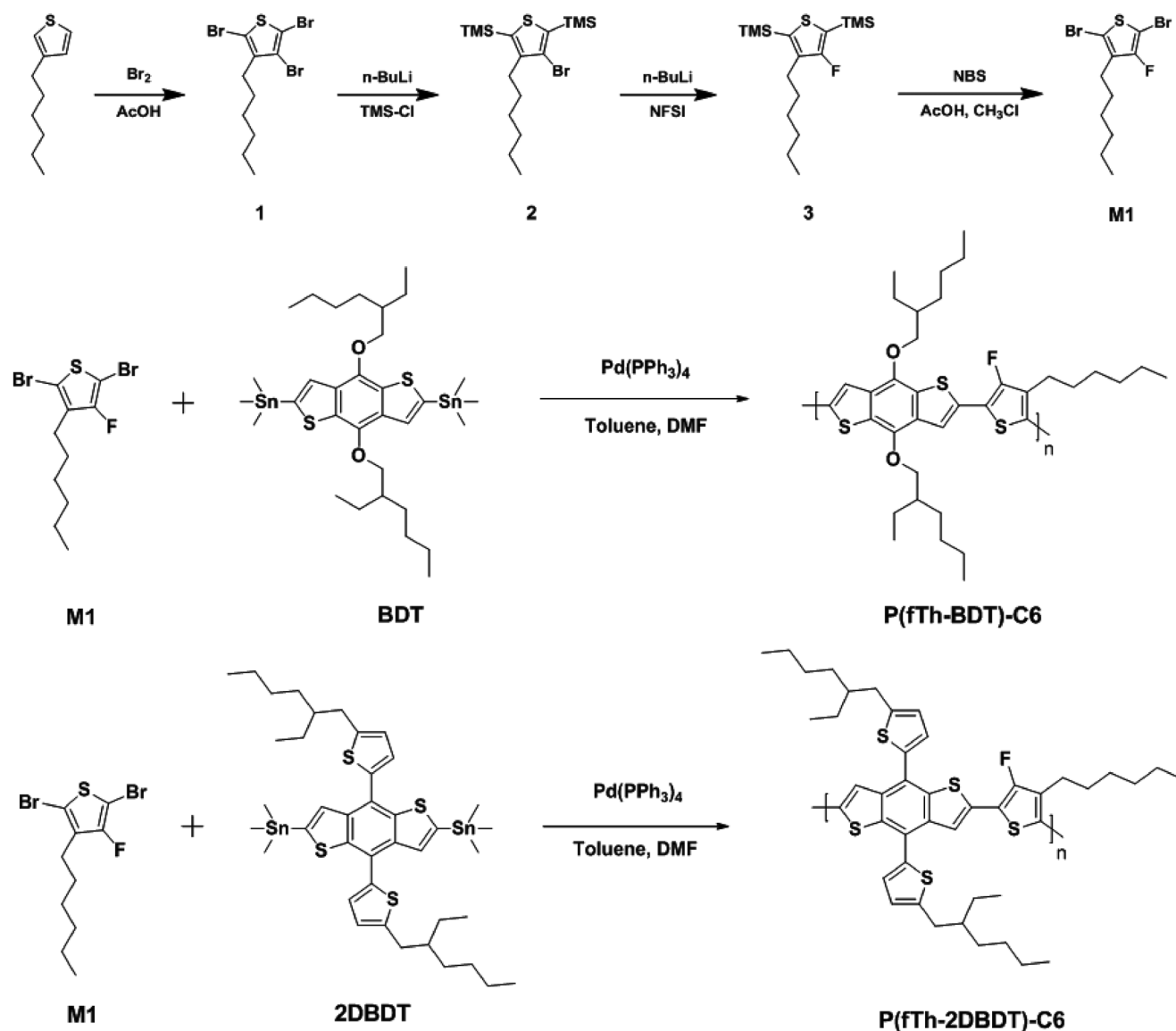
However, fluorinated polymers exhibit increased backbone rigidity, causing strong aggregation of molecules that limits their solubility in common organic solvents.^[34–36] The solubility of donor polymers is essential for solution processability and forming appropriate nanoscale bicontinuous interpenetrating networks to achieve high charge-carrier mobility.^[37,38] Introducing long alkyl chains improves polymer solubility in common organic solvents by modulating the intermolecular π - π interchain interactions. However, if the solubility and intermolecular interactions of the polymers are not properly balanced, the decrease in molecular weight due to poor π - π interchain interactions may interfere with the transport of charge carriers. Therefore, selecting chains of appropriate length and bulkiness is very important for designing donor polymers.^[39] Li and co-workers synthesized three types of polymers using a backbone composed of BDT and Th, to which fluorine, 2-hexyldecyl (HD), 2-octyl-dodecyl (OD), and 2-decyltetradecyl (DT) chains were introduced. The study reported that as the length of the chain increased, the molecular weight increased and the molecular packing changed. As a result, HD-PBDT2FT with appropriate length and bulkiness was obtained, and its PCE was 8.7%.^[40]

Therefore, in this study, we achieve optimal performance for BDT- and Th-based polymers by simultaneously introducing fluorine and alkyl side chain. Using this technique, we designed and synthesized two D-A type WBG donor polymers, P(fTh-BDT)-C6 and P(fTh-2DBDT)-C6, which exhibited good properties, such as oxidation stability and high charge-carrier mobility. Also, the polymers presented good solubility in common chlorinated solvents and nonhalogenated solvents, enabling eco-friendly processing. In brief, a blend film of P(fTh-2DBDT)-C6:ITIC-Th as active layer for OSCs was prepared using chlorobenzene (CB) as halogenated solvent and 1,8-diiodooctane (DIO) as halogenated additive. The corresponding OSC device presented a maximum PCE of 11.1%, an open-circuit voltage, V_{OC} , of 0.94 V, a short-circuit current density, J_{SC} , of 17.1 mA cm⁻², and a fill factor, FF, of 62.8%. In addition, when *o*-xylene and diphenyl ether (DPE) were used as nonchlorinated solvent and nonhalogenated additive, respectively, we obtained an OSC device with a high PCE of 10.9%, V_{OC} of 0.92 V, J_{SC} of 17.3 mA cm⁻², and FF of 68.4%. Both devices exhibited excellent long-term stability and their efficiencies increased by 100% and 101% after 1272 and 768 h of stability measurements, respectively. The results of this study indicated that donor polymers modified using the simultaneous fluorination and alkylation technique were effective for producing high-performance NFOSCs. Moreover, this report offers interesting information on the molecular design of D-A polymers for NFOSCs.

Scheme 1 illustrates the synthesis reactions of the monomers and polymers in this study. The synthesis of 2, 5-dibromo-3-fluoro-4-hexylthiophene (M1) and polymerization of poly[[4,8-bis[5-(2-ethylhexyl)oxy]benzo[1,2-*b*:4,5-*b'*]dithiophene-2,6-diyl]-(3-fluoro-4-hexylthiophene)] and P(fTh-BDT)-C6 using poly[[4,8-bis[5-(2-ethylhexyl)-2-thienyl]benzo[1,2-*b*:4,5-*b'*]dithiophene-2,6-diyl]-(3-fluoro-4-hexylthiophene)] and P(fTh-2DBDT)-C6 were performed using modified methods reported in previous studies.^[41] The polymerization reactions are described in Experimental Section. As illustrated in Scheme 1, the synthesis of M1 consisted of four steps, and a viscous pale yellow liquid was obtained as the final product. Details of the synthesis process and characterization data are presented in the Supporting Information. The polymers were obtained using Stille coupling polymerization between M1 and BDT or 2DBDT. Soxhlet purification was performed to prevent burn-in-loss of the devices using methanol (MeOH), acetone (Ace), hexane (Hxn), Hxn:1,2-dichloropropane (DCP), ethyl acetate (EA), chloroform (CF), and DCP in this particular order.^[42] Most of the P(fTh-BDT)-C6 polymers were obtained starting with the Hxn fraction and the P(fTh-2DBDT)-C6 polymers were obtained using the CF fraction. The molecular structures of the obtained polymers were confirmed using NMR spectroscopy and elemental analysis (EA) (see Figures S1–S6 in the Supporting Information). In addition, the physical properties of the synthesized polymers were measured using thermogravimetric analysis (TGA) and gel permeation chromatography (GPC) (see Figures S7, S8 and Table S1 in the Supporting Information). Introducing fluorine into P(fTh-BDT)-C6 and P(fTh-2DBDT)-C6 resulted in good thermal stability and 5% weight loss temperatures (T_d , 5% weight loss) of 315 and 346 °C, respectively.^[43] The number-average molecular weight (M_n) values of P(fTh-BDT)-C6 and P(fTh-2DBDT)-C6 were 2 and 67 kDa, and the polydispersity indices (PDI) were 14.50 and 3.00, respectively.

Theoretical simulations of the two polymers were performed using density functional theory (DFT) at the B3LYP/6-31G(d) level (see Figure S9 in the Supporting Information). Two donor polymers, P(fTh-BDT)-C6 and P(fTh-2DBDT)-C6 featured a dihedral angle of 0° between the BDT core and fluorinated thiophene. The inter/intramolecular interactions exerted by these fluorine substituents (e.g., F...H, F...S, F... π) can have a considerable effect on the polymer backbone planarity and stacking of these conjugated materials in the solid state.^[44] Furthermore, P(fTh-BDT)-C6 with an alkoxy chain featured a dihedral angle of 91.32° between the BDT core and alkoxy chain, while P(fTh-2DBDT)-C6 featured a lower dihedral angle of 57.73° between the BDT core and alkylthienyl side chain, and thus, its backbone was more planar compared to that of the P(fTh-BDT)-C6 with an alkoxy chain. Therefore, we predicted that P(fTh-2DBDT)-C6 can form stronger π - π stacking than P(fTh-BDT)-C6 in solid thin films.^[45]

Due to the relatively small size of fluorine, we expected that disruptive steric interactions would be minimized, while the strong electron withdrawing nature of fluorine could cause an increase in inter- and intramolecular packing.^[46] However, these properties of fluorine may reduce the solubilities of the polymers.^[47] To prevent the decrease in solubility, we simultaneously introduced fluorine atoms and hexyl chains to the backbone of the polymer. Because the hexyl chains present appropriate



Scheme 1. Synthesis of P(fTh-BDT)-C6 and P(fTh-2DBDT)-C6.

lengths and bulkiness, we expected that the polymers would present good solubility and high molecular interactions. Both polymers were highly soluble in halogenated solvents such as CF and CB, as well as common nonchlorinated organic solvents such as toluene, *o*-xylene, and tetrahydrofuran (THF), and thus they would be suitable for eco-friendly processes.^[37]

Figure 1a illustrates the UV-vis absorption spectra of CF solutions of the polymers and Figure 1b presents the spectra of the spin-coated thin-film polymers and ITIC-Th. And UV-vis absorption spectra of the polymers and ITIC-Th in solutions and thin films are shown in Figure S10 in the Supporting Information, respectively. As shown in Figure 1a and Figure S11 in the Supporting Information, the molar absorption coefficients (ϵ) of P(fTh-BDT)-C6 and P(fTh-2DBDT)-C6 were $54\,215$ and $63\,333\ \text{M}^{-1}\ \text{cm}^{-1}$ at λ_{max} of 493 and 510 nm, respectively. Both polymers presented reasonable molar absorption coefficient values, which were higher than $50\,000$, indicating

an exceptional potential for harvesting solar photons and high J_{SC} values.^[48]

Both polymers exhibited absorption peaks in the $320\text{--}650$ nm range (Figure 1b), which indicated complementary UV-vis absorption with ITIC-Th, which presented absorption peaks in the wavelength range $500\text{--}780$ nm. Moreover, the polymers:ITIC-Th blended films displayed efficient light harvesting properties.^[49] The main absorption peaks of the thin polymers films redshifted and exhibited broader absorption peaks compared to those of the polymers in solution. This occurred because the chains of the thin fluorinated polymers films were likely to have been packed more closely compared to the polymers in solution, thus resulting in aggregation and enhanced intermolecular charge transfer (ICT).^[50]

P(fTh-BDT)-C6 presented only 0–1 absorption peaks in the $320\text{--}650$ nm range and no 0–2 or 0–0 absorption peaks. As the alkoxy side chains influenced the tilting angle between D–A,

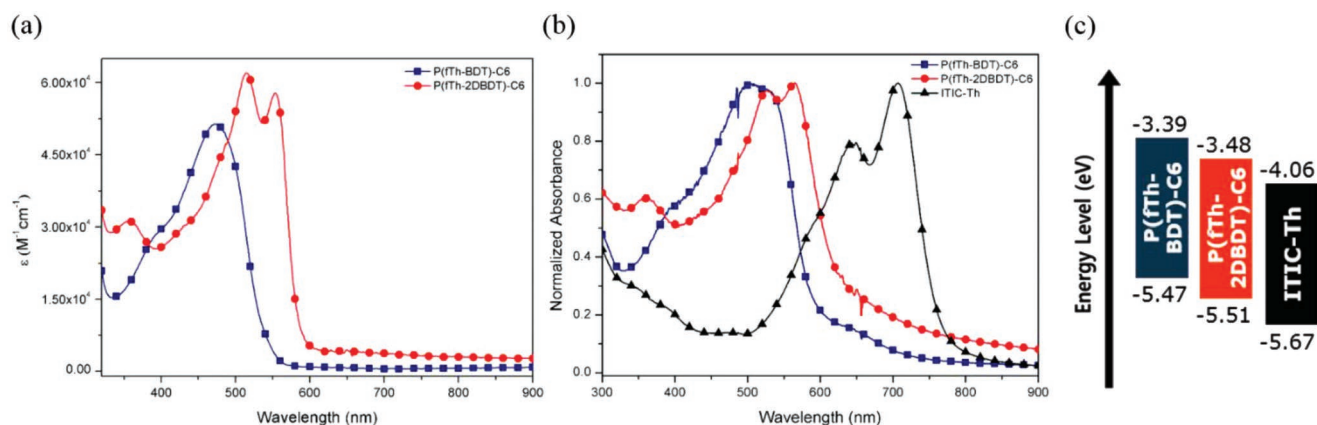


Figure 1. a) Average molar absorption coefficient in different dilute CF solutions. b) UV-vis absorption spectra of thin film on quartz plate from CF solutions. c) Energy level diagrams of the polymers and ITIC-Th.

the ICT and crystallinity values decreased.^[5,51] P(fTh-2DBDT)-C6 presented a 0–2 absorption peak (π – π^* transitions) in the 350–500 nm range and 0–1 and 0–0 absorption peaks in the 500–650 nm range.^[52] The backbone of P(fTh-2DBDT)-C6 was more planar compared to that of P(fTh-BDT)-C6; therefore, it promoted stronger inter- and intramolecular charge-transfer interactions.^[53]

The electrochemical properties of the polymers were measured using cyclic voltammetry (CV), and the results are illustrated in Figure S12 in the Supporting Information and Table 1. Figure 1c depicts the energy-level diagrams of the polymers and ITIC-Th. The optical bandgaps (E_g) of P(fTh-BDT)-C6 and P(fTh-2DBDT)-C6 were 2.08 and 2.03 eV, respectively, and the HOMO/lowest unoccupied molecular orbital (LUMO) energy levels were –5.47/–3.39 and –5.51/–3.48 eV, respectively. The fluorine substituents lowered the HOMO energy levels of both polymers, which contributed to the higher V_{OC} values of NFOSCs.^[54,55] In addition, the LUMO energy levels of the two polymers were considerably higher than that of ITIC-Th, thus contributing to a sufficiently high driving force for the dissociation of excitons.^[56]

We fabricated and characterized OSC devices to investigate the photovoltaic properties of the polymers. All fabricated devices exhibited the following inverted-cell structure: indium tin oxide (ITO) glass/zinc oxide (ZnO)/polymer:ITIC-Th/MoO₃/Ag.

The processing conditions for the active layer, such as the D/A ratio and thermal annealing temperature and time, were optimized to achieve optimal photovoltaic performances (see

Tables S2 and S3 in the Supporting Information). The current density–voltage (J – V) curves of the polymers are illustrated in Figure 2a and the corresponding photovoltaic parameters are summarized in Table 2.

The optimized D/A ratio was 1:1.5 for both polymers when CB and DIO were used as processing solvent and additive, respectively. The P(fTh-BDT)-C6 based OSC device exhibited a very low PCE of 1.1%. By contrast, the best P(fTh-2DBDT)-C6 device exhibited a remarkably high PCE of 11.1% and V_{OC} , J_{SC} , and FF of 0.92 V, 17.1 mA cm^{–2}, and 62.8%, respectively. The V_{OC} values of the two devices were 0.92 and 0.94 V, respectively, corresponding to the difference between the HOMO energy levels of each polymer and LUMO energy levels of ITIC-Th. Introducing fluorine into the two polymers lowered the HOMO energy level and increased V_{OC} .^[44] Furthermore, the parameters of the best P(fTh-2DBDT)-C6 device were higher than those of the P(fTh-BDT)-C6 device. This was due to the good phase separation which occurred in the active layer because of the broadened absorption and higher mobility of the 2D-conjugated BDT polymers.^[53]

The corresponding external quantum efficiency (EQE) curves of the devices fabricated using optimal polymers:ITIC-Th blends are illustrated in Figure 2b, and demonstrated that both devices absorb light over a wide wavelength range of 300–750 nm. However, as can be in Figure 2b, EQE was >20% in the 560–720 nm range and reached only 23% at the maximum wavelength of 700 nm. On the other hand, EQE of the P(fTh-2DBDT)-C6:ITIC-Th blend was >60% in the 520–710 nm range, and presented a maximum value of 71% at 660 nm. This

Table 1. Optical and electrochemical properties of polymers.

Polymer	Abs. [nm]		ϵ [M ^{–1} cm ^{–1}]	E_{onset} [eV]	$E_g^{Opt,a)}$ [eV]	HOMO ^{b)} [eV]	LUMO ^{b)} [eV]
	$\lambda_{max}^{Solution}$	λ_{max}^{Film}					
P(fTh-BDT)-C6	493	501	5.42×10^4	–1.16	2.08	–5.47	–3.39
P(fTh-2DBDT)-C6	350, 510	358, 519, 552	6.33×10^4	–1.20	2.03	–5.51	–3.48
ITIC-Th	670	635, 695	2.02×10^5	–1.36	1.61	–5.67	–4.06

^{a)} Calculated from the intersection of the tangent to the low energetic edge of the absorption spectrum with the baseline; ^{b)} E_{HOMO} (or LUMO) = $-[E_{onset}(vs Ag/AgCl) - E_{1/2}(Fc/Fc^+ vs Ag/AgCl)] - 4.8$ [eV] $E_{1/2}(Fc/Fc^+ vs Ag/AgCl) = 0.49$ eV (measured data).

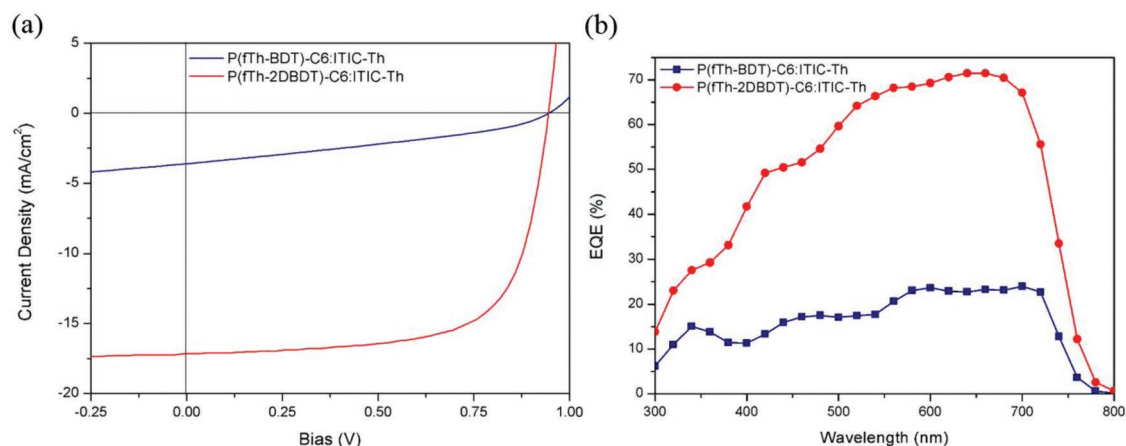


Figure 2. a) J - V and b) EQE curves of OSC devices processed using CB/DIO.

was consistent with the J_{SC} values from the photovoltaic performance measurements.

X-ray diffraction (XRD) measurements were performed to observe the crystallinity and molecular orientations of the two polymers (see Figure S13 and Table S4 in the Supporting Information). As shown in Figure S13a in the Supporting Information, the out-of-plane direction of pristine P(fTh-BDT)-C6 film presented a (100) peak, which was related to the lamellar appearance at $2\theta = 5.19^\circ$. For pristine P(fTh-2DBDT)-C6, the (100) peak was not observed, but the broad (010) peak associated with π - π stacking appeared at $2\theta \approx 21.90^\circ$. According to Bragg's law ($\lambda = 2d\sin\theta$), the lamellar distance of P(fTh-BDT)-C6 is 16.99 Å, and the π - π stacking distance of P(fTh-2DBDT)-C6 is 4.05 Å. This indicated that the edge-on tendency was dominant in P(fTh-BDT)-C6, as shown in Figure S13e in the Supporting Information, and the face-on tendency was dominant in P(fTh-2DBDT)-C6, as shown in Figure S13f in the Supporting Information. In addition, we measured the crystallinities of the polymers and nonfullerene acceptor-blended thin films, as shown in Figure S13c,d in the Supporting Information. Figure S13c in the Supporting Information illustrates the out-of-plane direction of the blended thin polymer films, where only the P(fTh-2DBDT)-C6 blend exhibited a $d_{(010)}$ peak at 3.54 Å. This revealed that P(fTh-2DBDT)-C6 maintained the face-on tendency even when blended with ITIC-Th, and the decrease in $d_{(010)}$ indicated improved π - π stacking.^[57,58] The face-on structure is more advantageous for the transfer of electric charge than the edge-on structure.^[59,60] These results were consistent with the photovoltaic properties of P(fTh-BDT)-C6 and P(fTh-2DBDT)-C6.

To confirm the good processability of P(fTh-2DBDT)-C6, we fabricated OSC devices using optimized ratios of eco-friendly solvents such as toluene and *o*-xylene in CB/DIO devices (see Table S5 in the Supporting Information), and the results are shown in Figure 3 and Table 2. As illustrated in Figure 3a, PCE was 10.4% while V_{OC} , J_{SC} , and FF were 0.94 V, 16.7 mA cm⁻², and 66.1%, respectively, when only *o*-xylene was used as processing solvent. When 0.5 vol% DPE was added to CB/DIO, PCE became 10.6% in *o*-xylene and 10.4% in toluene. Moreover, after adding 0.25 vol% DPE to *o*-xylene, the highest PCE of 10.9% was achieved, while V_{OC} , J_{SC} , and FF were 0.92 V, 17.4 mA cm⁻², and 68.4%, respectively. This indicated that P(fTh-2DBDT)-C6 fabricated using the simultaneously fluorination and alkylation technique could be a promising donor polymer for practical application because of its high PCE and environment friendly fabrication process.^[61] Additionally, the *o*-xylene-processed device achieved a high performance without using any solvent additives or post-treatments, which could greatly simplify the fabrication of OSC devices.^[62]

Figure 3b shows that both devices absorb light in the wide 300–750 nm range. When using *o*-xylene and *o*-xylene/DPE as processing solvents, the maximum EQEs at 680 nm were 71% and 68%, respectively. The calculated J_{SC} presented the same tendency as those of the devices listed in Table 2.

To further understand the difference in efficiency, we examined the fluorescence quenching of the polymers when mixed with ITIC-Th through photoluminescence (PL) measurements (see Figure S14 in the Supporting Information). The films were excited at their maximum absorptions. Each spectrum was corrected for the absorption of the film at the excitation

Table 2. Photovoltaic performances of polymers:ITIC-Th under AM 1.5G illumination, 100 mW cm⁻².

Polymer	Solvents/additives	V_{OC} [V]	J_{SC} [mA cm ⁻²]	FF [%]	PCE _{max} [%]	PCE _{ave} ^{a)} [%]
P(fTh-BDT)-C6	CB/DIO ^{b)}	0.92	3.2	33.5	1.1	0.6
P(fTh-2DBDT)-C6	CB/DIO ^{b)}	0.94	17.1	62.8	11.1	10.6
P(fTh-2DBDT)-C6	<i>o</i> -xylene ^{c)}	0.94	16.7	66.1	10.4	10.3
P(fTh-2DBDT)-C6	<i>o</i> -xylene/DPE ^{b)}	0.92	17.3	68.4	10.9	10.6

^{a)}The average PCE values were calculated using 10 independent cells; ^{b)}Subjected to thermal annealing at 110 °C for 10 min; ^{c)}As-cast without any post-treatments.

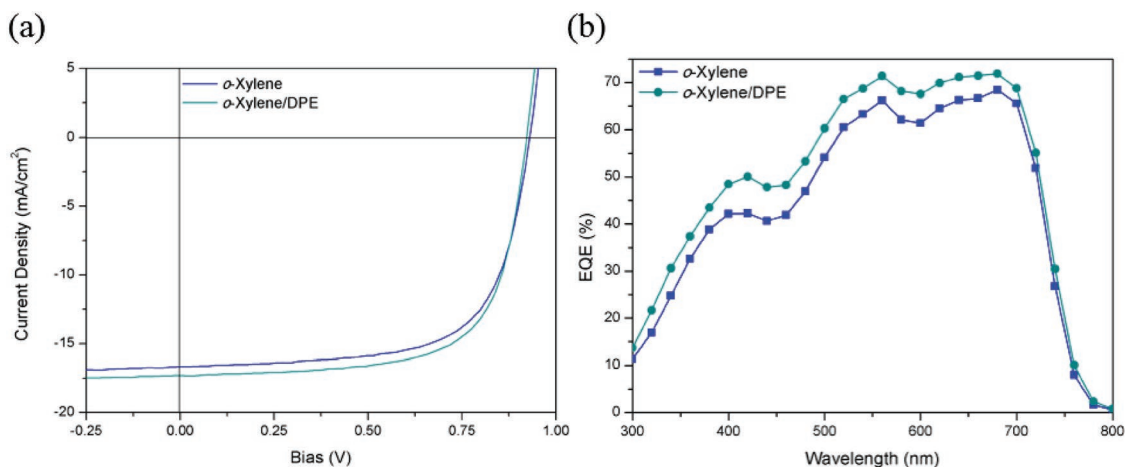


Figure 3. a) J - V and b) EQE curves of P(fTh-2DBDT)-C6:ITIC-Th-based devices processed using eco-friendly solvents.

wavelength. As shown in Figure S14a,b in the Supporting Information, the P(fTh-BDT)-C6, P(fTh-2DBDT)-C6, and ITIC-Th films presented strong PL emissions in the 700–850, 600–800, and 700–850 nm ranges, respectively. Both blended films exhibited similar behavior which involved PL quenching in the ITIC-Th film. However, for the donor polymers, the PL quenching efficiencies of the P(fTh-BDT)-C6 and P(fTh-2DBDT)-C6 blended films were 63% and 85%, respectively. This indicated that the electron transfer from the polymers to ITIC-Th for the excitons generated in the donor phase was more effective in the P(fTh-2DBDT)-C6 blended film than in the P(fTh-BDT)-C6 blended film.^[63]

Figure S14c in the Supporting Information illustrates the PL spectra of P(fTh-2DBDT)-C6 and ITIC-Th films using *o*-xylene and *o*-xylene/DPE as processing solvents. The PL values of the donor polymers and acceptors were 75% and 45% quenched, respectively, by the P(fTh-2DBDT)-C6 blended film. When DPE was added, the PL values of the donor polymers and acceptors were 76% and 46% quenched. These values were slightly higher than those obtained when using *o*-xylene alone. These results were consistent with the trends exhibited by the photovoltaic properties of the polymers.

To improve our understanding of the performance of the OSCs, we measured the electron and hole mobilities using a space-charge-limited current (SCLC) method, and the results are shown in **Figure 4** and **Table 3**. Hole-only devices with ITO/PEDOT:PSS/polymer:ITIC-Th/MoO₃/Ag structures, and electron-only devices with ITO/ZnO/polymer:ITIC-Th/LiF/Al structures were fabricated.

As shown in Table 3, the electron/hole mobility of the P(fTh-BDT)-C6-based device was $7.50 \times 10^{-5} \text{ cm}^2 \text{ V}^{-1} \text{ s}^{-1}$ / $9.82 \times 10^{-7} \text{ cm}^2 \text{ V}^{-1} \text{ s}^{-1}$. Thus, the difference in mobility was more than two orders of magnitude and μ_e/μ_h was 76.37. The electron/hole mobility of P(fTh-2DBDT)-C6-based devices was higher ($1.50 \times 10^{-4} \text{ cm}^2 \text{ V}^{-1} \text{ s}^{-1}$ / $1.12 \times 10^{-5} \text{ cm}^2 \text{ V}^{-1} \text{ s}^{-1}$) and their charge balance was superior compared to P(fTh-BDT)-C6.^[64] These differences in values originate in the planarity of the backbone of the polymer and microstructural ordering. Moreover, these differences explained why the P(fTh-2DBDT)-C6-based devices presented superior J_{SC} and FF values.^[65] In addition, when *o*-xylene and *o*-xylene/DPE were used as processing solvents, the electron/hole mobilities were $1.12 \times 10^{-4} \text{ cm}^2 \text{ V}^{-1} \text{ s}^{-1}$ / $2.13 \times 10^{-5} \text{ cm}^2 \text{ V}^{-1} \text{ s}^{-1}$ and $2.10 \times 10^{-4} \text{ cm}^2 \text{ V}^{-1} \text{ s}^{-1}$ / $4.19 \times 10^{-5} \text{ cm}^2 \text{ V}^{-1} \text{ s}^{-1}$, and μ_e/μ_h were

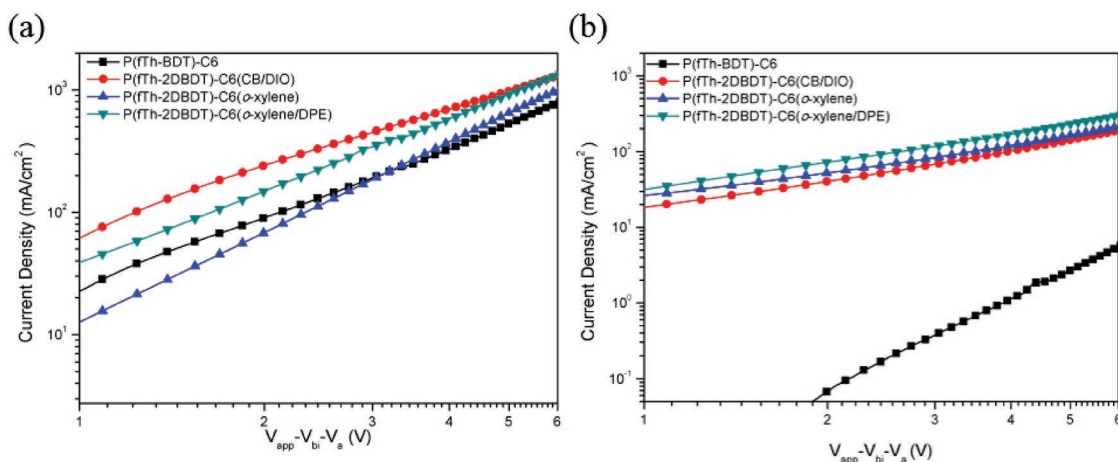


Figure 4. J_{ph} - V curves of a) electron-only and b) hole-only devices for polymers:ITIC-Th blended films.

Table 3. Electron and hole mobilities (μ_e and μ_h) of polymers measured using the SCLC method.

Conditions	μ_e [$\text{cm}^2 \text{V}^{-1} \text{s}^{-1}$]	μ_h [$\text{cm}^2 \text{V}^{-1} \text{s}^{-1}$]	μ_e/μ_h
P(fTh-BDT)-C6:ITIC-Th ^{a)}	7.50×10^{-5}	9.82×10^{-7}	76.37
P(fTh-2DBDT)-C6:ITIC-Th ^{a)}	1.50×10^{-4}	1.12×10^{-5}	13.39
P(fTh-2DBDT)-C6:ITIC-Th ^{b)}	1.12×10^{-4}	2.13×10^{-5}	5.25
P(fTh-2DBDT)-C6:ITIC-Th ^{c)}	2.10×10^{-4}	4.19×10^{-5}	5.01

^{a)}Processed using CB/DIO; ^{b)}Processed using *o*-xylene; ^{c)}Processed using *o*-xylene/DPE.

5.25 and 5.10, respectively. The balance ratios of μ_e/μ_h when *o*-xylene and *o*-xylene/DPE were used as processing solvents were higher than those obtained when CB/DIO was used as processing solvent in P(fTh-2DBDT)-C6-based devices. This was consistent with the tendency of FF to increase.

To investigate the phase separation morphologies of the polymer:ITIC-Th blends, atomic force microscopy (AFM) analysis and transmission electron microscopy (TEM) analysis were performed, and the results are shown in **Figure 5** and **Figure S15** in the Supporting Information. In the AFM topographic images in **Figure 5**, light and dark domains appeared as the polymer and ITIC-Th were aggregated. When CB/DIO was used as solvent, the root-mean-square roughness (RMS) values of the P(fTh-BDT)-C6 and P(fTh-2DBDT)-C6 blended films in **Figure 5a** and **b** were 4.23 and 1.59, respectively. These RMS values might have been related to the strong π - π inter-chain interaction and self agglomeration.^[66] The large RMS and large domain size of the P(fTh-BDT)-C6 blended film impaired the charge-carrier transport.^[67] This further explained the weaker EQE response of the P(fTh-BDT)-C6 blended film. Furthermore, the TEM images show that the morphology of the

P(fTh-2DBDT)-C6 blended film was more clear and uniform than P(fTh-BDT)-C6. It provides not only a suitable domain size for efficient exciton dissociation but also a continuous interpenetrating network for transporting charge carriers in the nanoscale. Large phase separations reduced the exciton diffusion/separation efficiencies, and finally led to OSCs characterized by low PCEs.^[9] The RMS values of the P(fTh-2DBDT)-C6 blended films in **Figure 5c** and **d** were 1.12 and 1.18 when *o*-xylene and *o*-xylene/DPE were used as processing solvents, respectively. And compared to the TEM images processed using CB/DIO, the P(fTh-2DBDT)-C6 blended film in **Figure 5g** presented relatively larger crystallite domain sizes, which could have arisen from the different solubilities of the blended films.^[68] The P(fTh-2DBDT)-C6 blended film in **Figure 5h** shows finer morphology than **Figure 5g** due to the presence of DPE additives.^[69] The internal morphology of the P(fTh-2DBDT)-C6 blended film processed by *o*-xylene/DPE was homogeneous, consisting of nanoscale segregated crystallites; this structure is known to favor effective exciton diffusion, charge separation, and transport because it promotes the formation of continuous charge-transport channels. The results indicated higher J_{SC} and FF values for the OSCs.

We measured the long-term stability of the optimized P(fTh-2DBDT):ITIC-Th-based device, and the results are illustrated in **Figure 6** and **Table S6** in the Supporting Information. **Figure 6** depicts the time-dependent changes in the PCE values of devices that used CB/DIO, *o*-xylene, and *o*-xylene/DPE as processing solvents. **Figure 6a** and **Table S6** in the Supporting Information demonstrate that the V_{OC} and J_{SC} of the device slightly decreased in time, while FF increased. The device processed using CB/DIO presented 100% efficiency after 1272 h compared to the initial efficiency, and those processed using *o*-xylene and *o*-xylene/DPE exhibited 94% and 101% efficiencies

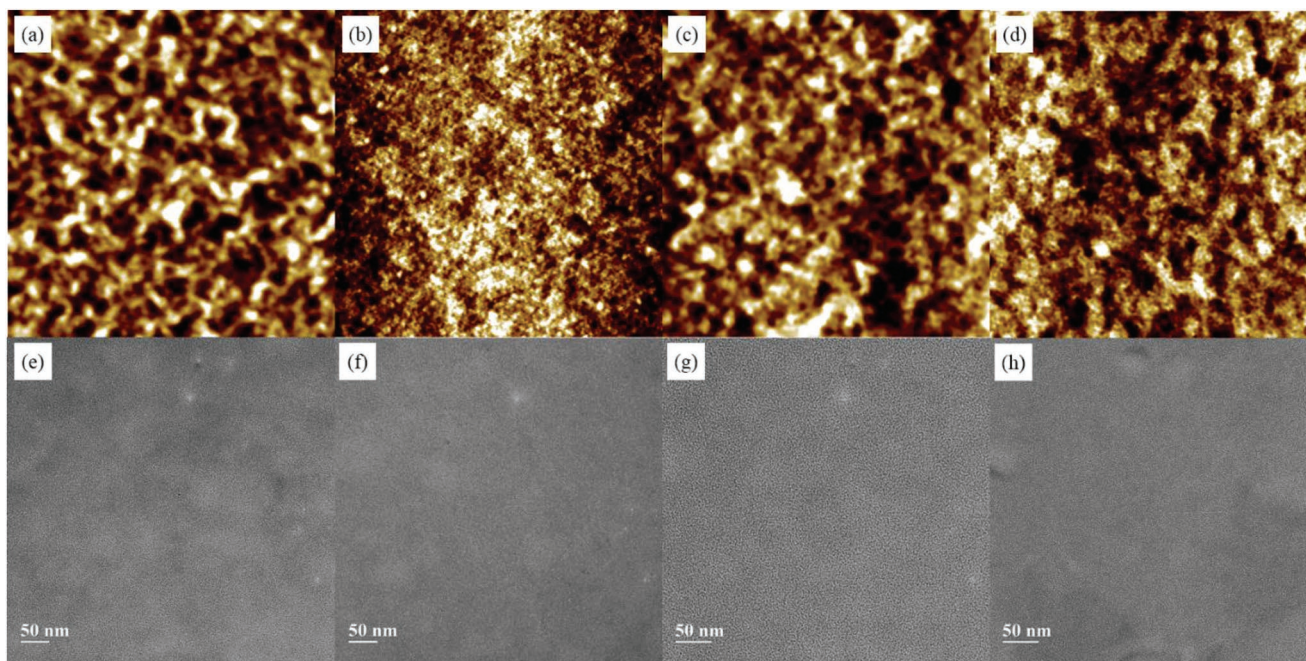


Figure 5. AFM topographic ($5 \mu\text{m} \times 5 \mu\text{m}$) and TEM images of blend films of a,e) P(fTh-BDT)-C6:ITIC-Th and b,f) P(fTh-2DBDT)-C6:ITIC-Th processed by CB/DIO, c,g) *o*-xylene and d,h) *o*-xylene/DPE.

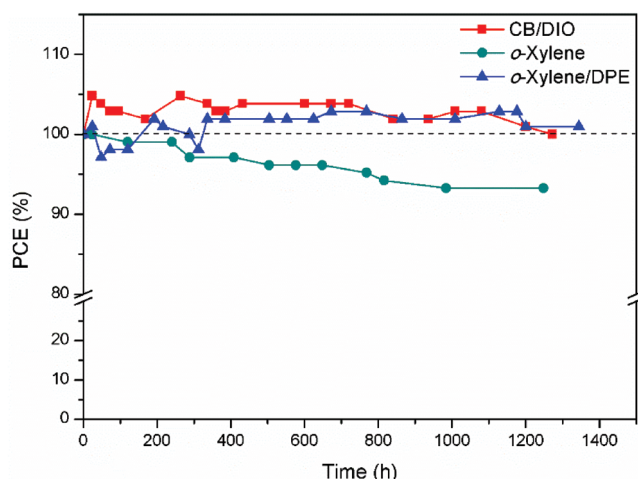


Figure 6. PCE-time graphs of P(fTh-2DBDT)-C6:ITIC-Th-based device using different solvents.

after 816 and 768 h, respectively. Although the tendency of the device processed using *o*-xylene was to present a slight decrease in long-term stability compared to those of the devices processed using other solvents, this device did not use any solvent additives and post-treatment. Therefore, the fabrication process of this device was simplified and did not require additional vacuum processing to remove additives. Thus, P(fTh-2DBDT)-C6 incorporating fluorine and hexyl chains presented excellent oxidation stability, and simultaneously exhibited good stability in both halogenated and nonhalogenated solvents.^[70,71]

Furthermore, we also kept the devices under continuous illumination (AM 1.5G illumination at 100 mW cm⁻²) without encapsulation to investigate the device operational stability. The device performance was measured periodically to observe the illumination-dependent degradation effect in the device performance for 2 h (See Figure S16 in the Supporting Information). And Figure S17 in the Supporting Information exhibits the change in the normalized photovoltaic parameters with the illumination time. It can be seen that the performance of all the devices decreased with increasing operation time; however, the P(fTh-2DBDT):ITIC-Th-based devices demonstrated good operational stability.^[68] For the device processed by *o*-Xylene and *o*-Xylene/DPE, its PCE retains 64% of its initial efficiency. However, the device processed by CB/DIO, its PCE dropped by 45% after 2 h of testing. It can be estimated that nonhalogenated solvents cause less damage to donor and acceptor materials in air with the light illumination because of the stable molecular structures of these solvents consisting of stable carbon and hydrogen atoms.^[72–74]

In this study, we designed and synthesized WBG donor polymers employing a simultaneous fluorination and alkylation technique using BDT-Th (D–A), P(fTh-BDT)-C6 and P(fTh-2DBDT)-C6 to produce highly efficient NFOSCs. By simultaneously introducing fluorine and alkyl chains into the polymers, both polymers achieved good balance between solubility and intermolecular interactions. Accordingly, they were determined to be suitable for fabricating highly efficient NFOSCs using nonchlorinated organic solvents. In particular, the inverted P(fTh-2DBDT)-C6 structure with high molecular

weight due to the planar backbone presented the highest PCE of 11.1% in the P(fTh-2DBDT)-C6:ITIC-Th blend when CB/DIO was used as processing solvent. P(fTh-2DBDT)-C6 also presented a PCE of 10.9% when *o*-xylene/DPE was used as processing solvent. To the best of our knowledge, the PCE of the P(fTh-2DBDT)-C6:ITIC-Th device was one of the highest for NFOSCs developed using eco-friendly solvents to date. In addition, P(fTh-2DBDT)-C6-based devices processed using CB/DIO maintained 100% efficiency after 1272 h, and the device processed using *o*-xylene/DPE presented a 101% increase in efficiency after 768 h, indicating excellent long-term stability. This demonstrated that the simultaneous fluorination and alkylation technique could be an effective method for fabricating donor polymers for NFOSCs with high performance sustainability.

Experimental Section

Materials: All reagents and chemicals were purchased from TCI Co., Sigma-Aldrich Co., and Acros Organics Co. and were used without further purification unless otherwise stated. The 2,6-bis(trimethyltin)-4,8-bis(2-ethylhexyloxy)benzo[1,2-*b*:4,5-*b'*]dithiophene (BDT) and (4,8-bis(4,5-didecylthiophen-2-yl)benzo[1,2-*b*:4,5-*b'*]dithiophene-2,6-diyl)bis(trimethylstannane) (2DBDT) were purchased from Suna Tech Inc.

Synthesis of P(fTh-BDT)-C6: A mixture of monomer M1 (34.4 mg, 0.1 mmol), BDT (76.85 mg, 0.0995 mmol), and tetrakis(triphenylphosphine)palladium(0) (5.77 mg, 0.005 mmol) was added to a 2–5 mL microwave vial in air. The vial was capped and vacuumed for 20 min, and then it was refilled with nitrogen gas, and subsequently, anhydrous toluene (3.0 mL) and anhydrous *N,N*-dimethylformamide (0.3 mL) were added to the mixture. Afterward, the reactor was degassed and refilled with nitrogen again. The polymerization mixture was stirred and was heated to reflux for 90 h. The polymer was end-capped by adding 2-bromothiophene (0.03 g, 0.177 mmol) and the mixture was further heated for 4 h at 110 °C. Subsequently, 2-tributylstannyl thiophene (0.017 g, 0.047 mmol) was added and the mixture was heated for 4 h at 110 °C. The reaction mixture was cooled to room temperature, poured into 300 mL MeOH, and further purified by Soxhlet extraction using MeOH, Ace, Hxn, EA, and CF. The Hxn fraction of the polymers was reprecipitated in MeOH, filtered, and dried under vacuum to yield P(fTh-BDT)-C6 (43 mg, yield: 69%) as a red solid. ¹H NMR (400 MHz, CDCl₃, δ): 7.69–6.85 (br, 2H), 4.42–3.85 (br, 4H), 3.00–2.33 (br, 2H), 1.93–1.22 (br, 22H), 1.22–0.70 (br, 14H), 0.95–0.84 (br, 18H). Anal. calcd. for C₃₅H₄₉FO₂S₃: C, 68.14; H, 8.01; F, 3.08; O, 5.19; S, 15.59; EA for C₃₅H₄₉FO₂S₃: C, 67.23; H, 7.68; O, 4.27; S, 14.35.

Synthesis of P(fTh-2DBDT)-C6: P(fTh-2DBDT)-C6 was synthesized following the same procedure used for synthesizing P(fTh-BDT)-C6. However, the final product was further purified by Soxhlet extraction using MeOH, Ace, Hxn, Hxn:DCP = 1:1, EA, and CF. The CF fraction of polymers was reprecipitated in MeOH, filtered, and dried under vacuum to yield P(fTh-2DBDT)-C6 (56 mg, yield: 73%) as a dark red solid. ¹H NMR (400 MHz, CDCl₃, δ): 7.81–7.48 (br, 2H), 7.38–7.28 (br, 2H), 7.16–6.83 (br, 2H), 3.07–2.84 (br, 4H), 2.84–2.46 (br, 2H), 1.85–1.65 (br, 2H), 1.65–1.14 (br, 24H), 1.14–0.74 (br, 15H). Anal. calcd. for C₄₆H₅₉FS₃: C, 69.82; H, 7.52; F, 2.40; S, 20.26; EA for C₄₆H₅₉FS₃: C, 69.56; H, 6.84; S, 19.29.

Supporting Information

Supporting Information is available from the Wiley Online Library or from the author.

Acknowledgements

This research was supported by the New and Renewable Energy Core Technology Program of the Korea Institute of Energy Technology Evaluation and Planning (KETEP) grant funded by the Ministry of Trade, Industry, and Energy, Republic of Korea (No. 20153010140030) the Korea Institute of Energy Technology Evaluation and Planning (KETEP) and the Ministry of Trade, Industry & Energy (MOTIE) of the Republic of Korea (2018201010636A) and the Human Resource Program in Energy Technology of the Korea Institute of Energy Technology Evaluation and Planning (KETEP) and the Ministry of Trade, Industry & Energy (MOTIE) of the Republic of Korea (Grant no. 20174010201540).

Conflict of Interest

The authors declare no conflict of interest.

Keywords

alkylation, eco-friendly, fluorination, nonfullerene, organic solar cells

Received: December 14, 2018

Published online:

- [1] G. Yu, J. Gao, J. C. Hummelen, F. Wudl, A. J. Heeger, *Science* **1995**, 270, 1789.
- [2] L. Meng, Y. Zhang, X. Wan, C. Li, X. Zhang, Y. Wang, X. Ke, Z. Xiao, L. Ding, R. Xia, H.-L. Yip, Y. Cao, Y. Chen, *Science* **2018**, 361, 1094.
- [3] X. Guo, N. Zhou, S. J. Lou, J. Smith, D. B. Tice, J. W. Hennek, R. P. Ortiz, J. T. L. Navarrete, S. Li, J. Strzalka, L. X. Chen, R. P. H. Chang, A. Facchetti, T. J. Marks, *Nat. Photonics* **2013**, 7, 825.
- [4] S. J. Jeon, S. J. Nam, Y. W. Han, T. H. Lee, D. K. Moon, *Polym. Chem.* **2017**, 8, 2979.
- [5] Y. Liu, J. Zhao, Z. Li, C. Mu, W. Ma, H. Hu, K. Jiang, H. Lin, H. Ade, H. Yan, *Nat. Commun.* **2014**, 5, 1.
- [6] Z. Xiao, X. Jia, L. Ding, *Sci. Bull.* **2017**, 62, 1562.
- [7] S. M. McAfee, J. M. Topple, I. G. Hill, G. C. Welch, *J. Mater. Chem. A* **2015**, 3, 16393.
- [8] Y. Lin, X. Zhan, *Mater. Horiz.* **2014**, 1, 470.
- [9] S. Holliday, R. S. Ashraf, C. B. Nielsen, M. Kirkus, J. A. Röhr, C. H. Tan, E. Collado-Fregoso, A. C. Knall, J. R. Durrant, J. Nelson, I. McCulloch, *J. Am. Chem. Soc.* **2015**, 137, 898.
- [10] Y. Lin, Y. Li, X. Zhan, *Chem. Soc. Rev.* **2012**, 41, 4245.
- [11] Z. Xiao, F. Liu, X. Geng, J. Zhang, S. Wang, Y. Xie, Z. Li, H. Yang, Y. Yuan, L. Ding, *Sci. Bull.* **2017**, 62, 1331.
- [12] D. Baran, T. Kirchartz, S. Wheeler, S. Dimitrov, M. Abdelsamie, J. Gorman, R. S. Ashraf, S. Holliday, A. Wadsworth, N. Gasparini, P. Kaienburg, H. Yan, A. Amassian, C. J. Brabec, J. R. Durrant, I. McCulloch, *Energy Environ. Sci.* **2016**, 9, 3783.
- [13] Z. Xiao, X. Jia, D. Li, S. Wang, X. Geng, F. Liu, J. Chen, S. Yang, T. P. Russell, L. Ding, *Sci. Bull.* **2017**, 62, 1494.
- [14] Y. Lin, J. Wang, Z.-G. Zhang, H. Bai, Y. Li, D. Zhu, X. Zhan, *Adv. Mater.* **2015**, 27, 1170.
- [15] Y. Lin, F. Zhao, Q. He, L. Huo, Y. Wu, T. C. Parker, W. Ma, Y. Sun, C. Wang, D. Zhu, A. J. Heeger, S. R. Marder, X. Zhan, *J. Am. Chem. Soc.* **2016**, 138, 4955.
- [16] S. Zhang, Y. Qin, J. Zhu, J. Hou, *Adv. Mater.* **2018**, 30, 1800868.
- [17] Y. Yang, Z. G. Zhang, H. Bin, S. Chen, L. Gao, L. Xue, C. Yang, Y. Li, *J. Am. Chem. Soc.* **2016**, 138, 15011.
- [18] D. Li, Z. Xiao, S. Wang, X. Geng, S. Yang, J. Fang, H. Yang, L. Ding, *Adv. Energy Mater.* **2018**, 8, 1800397.
- [19] L. Ye, Y. Xiong, S. Li, M. Ghasemi, N. Balar, J. Turner, A. Gadisa, J. Hou, B. T. O'Connor, H. Ade, *Adv. Funct. Mater.* **2017**, 27, 1702016.
- [20] H. Li, Z. Xiao, L. Ding, J. Wang, *Sci. Bull.* **2018**, 63, 340.
- [21] J. Wolf, F. Cruciani, A. El Labban, P. M. Beaujuge, *Chem. Mater.* **2015**, 27, 4184.
- [22] C. Roy, T. Bura, S. Beaupré, M. A. Légaré, J. P. Sun, I. G. Hill, M. Leclerc, *Macromolecules* **2017**, 50, 4658.
- [23] W. Li, S. Albrecht, L. Yang, S. Roland, J. R. Tumbleston, T. McAfee, L. Yan, M. A. Kelly, H. Ade, D. Neher, W. You, *J. Am. Chem. Soc.* **2014**, 136, 15566.
- [24] H. J. Son, W. Wang, T. Xu, Y. Liang, Y. Wu, G. Li, L. Yu, *J. Am. Chem. Soc.* **2011**, 133, 1885.
- [25] J. Warnan, A. El Labban, C. Cabanetos, E. T. Hoke, P. K. Shukla, C. Risko, J. L. Brédas, M. D. McGehee, P. M. Beaujuge, *Chem. Mater.* **2014**, 26, 2299.
- [26] R. Duan, L. Ye, X. Guo, Y. Huang, P. Wang, S. Zhang, J. Zhang, L. Huo, J. Hou, *Macromolecules* **2012**, 45, 3032.
- [27] S. Zhang, L. Ye, Q. Wang, Z. Li, X. Guo, L. Huo, H. Fan, J. Hou, *J. Phys. Chem. C* **2013**, 117, 9550.
- [28] H. Zhou, L. Yang, W. You, *Macromolecules* **2012**, 45, 607.
- [29] Y. Lin, F. Zhao, Y. Wu, K. Chen, Y. Xia, G. Li, S. K. K. Prasad, J. Zhu, L. Huo, H. Bin, Z. G. Zhang, X. Guo, M. Zhang, Y. Sun, F. Gao, Z. Wei, W. Ma, C. Wang, J. Hodgkiss, Z. Bo, O. Inganäs, Y. Li, X. Zhan, *Adv. Mater.* **2017**, 29, 1604155.
- [30] F. Babudri, G. M. Farinola, F. Naso, R. Ragni, *Chem. Commun.* **2007**, 0, 1003.
- [31] D. Mo, H. Wang, H. Chen, S. Qu, P. Chao, Z. Yang, L. Tian, Y. A. Su, Y. Gao, B. Yang, W. Chen, F. He, *Chem. Mater.* **2017**, 29, 2819.
- [32] K. Reichenbacher, H. I. Süss, J. Hulliger, *Chem. Soc. Rev.* **2005**, 34, 22.
- [33] Y. Firdaus, L. P. Maffei, F. Cruciani, M. A. Müller, S. Liu, S. Lopatin, N. Wehbe, G. O. N. Ndjawa, A. Amassian, F. Laquai, P. M. Beaujuge, *Adv. Energy Mater.* **2017**, 7, 1700834.
- [34] Y. Li, J. Zou, H. L. Yip, C. Z. Li, Y. Zhang, C. C. Chueh, J. Intemann, Y. Xu, P. W. Liang, Y. Chen, A. K. Y. Jen, *Macromolecules* **2013**, 46, 5497.
- [35] C. B. Nielsen, A. J. P. White, I. McCulloch, *J. Org. Chem.* **2015**, 80, 5045.
- [36] N. Leclerc, P. Chávez, O. A. Ibraikulov, T. Heiser, P. Lévêque, *Polymers* **2016**, 8, 11.
- [37] S. Li, B. Zhao, Z. He, S. Chen, J. Yu, A. Zhong, R. Tang, H. Wu, Q. Li, J. Qin, Z. Li, *J. Mater. Chem. A* **2013**, 1, 4508.
- [38] J. Yuan, Z. Zhai, H. Dong, J. Li, Z. Jiang, Y. Li, W. Ma, *Adv. Funct. Mater.* **2013**, 23, 885.
- [39] H. Yao, L. Ye, H. Zhang, S. Li, S. Zhang, J. Hou, *Chem. Rev.* **2016**, 116, 7397.
- [40] D. Xia, Y. Wu, Q. Wang, A. Zhang, C. Li, Y. Lin, F. J. M. Colberts, J. J. Van Franeker, R. A. J. Janssen, X. Zhan, W. Hu, Z. Tang, W. Ma, W. Li, *Macromolecules* **2016**, 49, 6445.
- [41] K. Nakabayashi, H. Otani, H. Mori, *Polym. J.* **2015**, 47, 617.
- [42] J. Kong, S. Song, M. Yoo, G. Y. Lee, O. Kwon, J. K. Park, H. Back, G. Kim, S. H. Lee, H. Suh, K. Lee, *Nat. Commun.* **2014**, 5, 1.
- [43] X. Liu, B. B. Y. Hsu, Y. Sun, C. K. Mai, A. J. Heeger, G. C. Bazan, *J. Am. Chem. Soc.* **2014**, 136, 16144.
- [44] Q. Zhang, L. Yan, X. Jiao, Z. Peng, S. Liu, J. J. Rech, E. Klump, H. Ade, F. So, W. You, *Chem. Mater.* **2017**, 29, 5990.
- [45] J. Cao, Q. Liao, X. Du, J. Chen, Z. Xiao, Q. Zuo, L. Ding, *Energy Environ. Sci.* **2013**, 6, 3224.
- [46] Z. Fei, P. Boufflet, S. Wood, J. Wade, J. Moriarty, E. Gann, E. L. Ratcliff, C. R. McNeill, H. Sirringhaus, J. S. Kim, M. Heaney, *J. Am. Chem. Soc.* **2015**, 137, 6866.
- [47] Y. Liang, Y. Luping, *Acc. Chem. Res.* **2010**, 43, 1227.
- [48] J. Yuan, M. J. Ford, Y. Zhang, H. Dong, Z. Li, Y. Li, T. Q. Nguyen, G. C. Bazan, W. Ma, *Chem. Mater.* **2017**, 29, 1758.

- [49] G. Zhang, X. Xu, Z. Bi, W. Ma, D. Tang, Y. Li, Q. Peng, *Adv. Funct. Mater.* **2018**, 28, 1.
- [50] S. Fukuta, J. Seo, H. Lee, H. Kim, Y. Kim, M. Ree, T. Higashihara, *Macromolecules* **2017**, 50, 891.
- [51] P. Guo, J. Sun, S. Sun, J. Li, J. Tong, C. Zhao, L. Zhu, P. Zhang, C. Yang, Y. Xia, *RSC Adv.* **2017**, 7, 22845.
- [52] B. Huang, L. Chen, X. Jin, D. Chen, Y. An, Q. Xie, Y. Tan, H. Lei, Y. Chen, *Adv. Funct. Mater.* **2018**, 28, 1800606.
- [53] J. Lee, J. H. Kim, B. Moon, H. G. Kim, M. Kim, J. Shin, H. Hwang, K. Cho, *Macromolecules* **2015**, 48, 1723.
- [54] Y. Li, L. Zhong, F.-P. Wu, Y. Yuan, H.-J. Bin, Z.-Q. Jiang, Z. Zhang, Z.-G. Zhang, Y. Li, L.-S. Liao, *Energy Environ. Sci.* **2016**, 9, 3429.
- [55] K. Zhang, Y. Qin, F. Li, L. Yu, M. Sun, *J. Phys. Chem. C* **2017**, 121, 19634.
- [56] W. Zhao, S. Zhang, Y. Zhang, S. Li, X. Liu, C. He, Z. Zheng, J. Hou, *Adv. Mater.* **2018**, 30, 1704837.
- [57] T. L. Nguyen, S. Song, S. J. Ko, H. Choi, J. E. Jeong, T. Kim, S. Hwang, J. Y. Kim, H. Y. Woo, *J. Polym. Sci., Part A: Polym. Chem.* **2015**, 53, 854.
- [58] M. An, F. Xie, X. Geng, J. Zhang, J. Jiang, Z. Lei, D. He, Z. Xiao, L. Ding, *Adv. Energy Mater.* **2017**, 7, 1602509.
- [59] M. H. Choi, H. Y. Kim, E. J. Lee, D. Kyung Moon, *Polymer* **2016**, 91, 162.
- [60] H. Y. Kim, M. H. Choi, Y. W. Han, D. K. Moon, J. R. Haw, *J. Ind. Eng. Chem.* **2016**, 33, 209.
- [61] D. Liu, B. Yang, B. Jang, B. Xu, S. Zhang, C. He, H. Y. Woo, J. Hou, *Energy Environ. Sci.* **2017**, 10, 546.
- [62] Y. An, X. Liao, L. Chen, J. Yin, Q. Ai, Q. Xie, B. Huang, F. Liu, A. K. Y. Jen, Y. Chen, *Adv. Funct. Mater.* **2018**, 28, 1706517.
- [63] H. Bin, Z. G. Zhang, L. Gao, S. Chen, L. Zhong, L. Xue, C. Yang, Y. Li, *J. Am. Chem. Soc.* **2016**, 138, 4657.
- [64] Q. Fan, Q. Zhu, Z. Xu, W. Su, J. Chen, J. Wu, X. Guo, W. Ma, M. Zhang, Y. Li, *Nano Energy* **2018**, 48, 413.
- [65] L. Yang, S. Zhang, C. He, J. Zhang, Y. Yang, J. Zhu, Y. Cui, W. Zhao, H. Zhang, Y. Zhang, Z. Wei, J. Hou, *Chem. Mater.* **2018**, 30, 2129.
- [66] S.-J. Ko, Q. V. Hoang, C. E. Song, M. A. Uddin, E. Lim, S. Y. Park, B. H. Lee, S. Song, S.-J. Moon, S. Hwang, P.-O. Morin, M. Leclerc, G. M. Su, M. L. Chabinyc, H. Y. Woo, W. S. Shin, J. Y. Kim, *Energy Environ. Sci.* **2017**, 10, 1443.
- [67] Z. Ji, X. Xu, G. Zhang, Y. Li, Q. Peng, *Nano Energy* **2017**, 40, 214.
- [68] G. E. Park, S. Choi, S. Y. Park, D. H. Lee, M. J. Cho, D. H. Choi, *Adv. Energy Mater.* **2017**, 7, 1700566.
- [69] S. J. Ko, Q. V. Hoang, C. E. Song, M. A. Uddin, E. Lim, S. Y. Park, B. H. Lee, S. Song, S. J. Moon, S. Hwang, P. O. Morin, M. Leclerc, G. M. Su, M. L. Chabinyc, H. Y. Woo, W. S. Shin, J. Y. Kim, *Energy Environ. Sci.* **2017**, 10, 1443.
- [70] S. Holliday, R. S. Ashraf, A. Wadsworth, D. Baran, S. A. Yousaf, C. B. Nielsen, C. H. Tan, S. D. Dimitrov, Z. Shang, N. Gasparini, M. Alamoudi, F. Laquai, C. J. Brabec, A. Salleo, J. R. Durrant, I. McCulloch, *Nat. Commun.* **2016**, 7, 1.
- [71] F. Gohier, P. Frère, J. Roncali, *J. Org. Chem.* **2013**, 78, 1497.
- [72] J. Zhao, S. Zhao, Z. Xu, D. Song, B. Qiao, D. Huang, Y. Zhu, Y. Li, Z. Li, Z. Qin, *ACS Appl. Mater. Interfaces* **2018**, 10, 24075.
- [73] S. Lee, J. Kong, K. Lee, *Adv. Energy Mater.* **2016**, 6, 1600970.
- [74] A. Wadsworth, R. S. Ashraf, M. Abdelsamie, S. Pont, M. Little, M. Moser, Z. Hamid, M. Neophytou, W. Zhang, A. Amassian, J. R. Durrant, D. Baran, I. McCulloch, *ACS Energy Lett.* **2017**, 2, 1494.